Am J Cancer Res 2026;16(7):2937-2954
www.ajcr.us /ISSN:2156-6976/ajcr0173972

Original Article

Correlation of tumor-infiltrating lymphocyte spatial distribution patterns with HER2 expression status and prognostic significance in gastric adenocarcinoma: a retrospective study based on digital pathology

Xinwu Mao, Shangwei Zhong, Xiaowen Zhang, Yuting Liu, Luqing Zhou

Department of Pathology, The First Affiliated Hospital of Lishui University, Lishui People's Hospital, Lishui 323000, Zhejiang, China

Received May 11, 2026; Accepted June 17, 2026; Epub July 15, 2026; Published July 30, 2026

Abstract: Background: The spatial distribution of tumor-infiltrating lymphocytes (TILs) has prognostic value in solid tumors, but its relationship with HER2 status in gastric adenocarcinoma remains poorly characterized. Methods: TIL densities in the tumor center (CT) and at the invasive margin (IM) were assessed on H&E-stained slides using QuPath, and the edge/center ratio (E/C ratio = IM-TILs/CT-TILs) was calculated. The optimal cut-off for E/C ratio was determined by maximizing the log-rank statistic. Survival analyses were performed using Kaplan-Meier and Cox regression. Results: The HER2-positive group (n = 35) exhibited significantly lower CT-TILs (11.92% vs. 20.98%, P < 0.001) and a higher E/C ratio (2.11 vs. 1.25, P < 0.001) than the HER2-negative group (n = 165). Using an optimal cut-off of 1.57, high E/C ratio was associated with significantly worse overall survival (OS) in the whole cohort (median 14.64 vs. 42.87 months; log-rank P < 0.001). Multivariate Cox regression, adjusting for clinicopathological factors, revealed that the E/C ratio as a continuous variable was independently prognostic (HR = 1.398, P < 0.001), and a significant interaction between HER2 status and E/C ratio was observed (HR = 1.844, P = 0.001). Dichotomization at E/C > 1.57 provides significant prognostic stratification, an effect that is modified by HER2 status; however, due to the small HER2-positive subgroup, these findings require validation in larger independent cohorts. Conclusions: HER2-positive gastric adenocarcinoma exhibits an "edge-limiting" immune phenotype with elevated E/C ratio. Digital assessment of TILs on routine H&E sections is simple and promising for clinical translation.

Keywords: Gastric adenocarcinoma, tumor-infiltrating lymphocytes, spatial distribution, HER2, digital pathology, prognosis

Introduction

Gastric cancer is the fifth most common malignancy worldwide and the third leading cause of cancer-related death. In 2020, there were over 1 million new cases and approximately 770,000 deaths worldwide [1, 2]. Gastric adenocarcinoma is the predominant histological type of gastric cancer, accounting for more than 90% of all gastric cancers. Despite significant advancements in surgical techniques, perioperative chemotherapy, and targeted therapy in recent years, the 5-year overall survival rate for advanced gastric cancer remains less than 30% [3, 4]. Therefore, finding reliable prognostic biomarkers and new therapeutic targets remain important topics in the field of gastric cancer research.

The human epidermal growth factor receptor 2 (HER2) is one of the earliest driver genes successfully targeted in gastric cancer. Approximately 15-20% of gastric adenocarcinomas exhibit HER2 protein overexpression or gene amplification [5, 6]. The ToGA study established the first-line treatment position of trastuzumab combined with chemotherapy in HER2-positive advanced gastric cancer [7-9]. However, subsequent multiple clinical studies have shown that anti-HER2 therapy combined with other drugs (such as pertuzumab, lapatinib, T-DM1) failed to replicate the significant benefits observed in

https://doi.org/10.62347/PEJP1288

breast cancer in gastric cancer, suggesting that the response to HER2-targeted therapy in gastric cancer may be deeply regulated by the tumor microenvironment (TME) [10-13]. Therefore, a deeper understanding of the immune microenvironment characteristics of HER2-positive gastric cancer is of great clinical significance for screening the optimal population for combined targeted/immunotherapy.

Tumor-infiltrating lymphocytes (TILs) directly reflect the host's adaptive immune response against tumors and are a core component of the tumor microenvironment (TME). Multiple large-scale studies and meta-analyses have confirmed that an increased density of TILs is significantly associated with a favorable prognosis in gastric cancer, especially in the EB virus-positive (EBV+) and microsatellite instability-high (MSI-H) subtypes, where TILs infiltration is more abundant and the response rate to immune checkpoint inhibitor therapy is higher [14, 15]. However, systematic research on the prognostic value and spatial distribution characteristics of TILs in HER2-positive gastric cancer is currently lacking. Previous few studies have found that $FoxP3^+$ regulatory T cells and M2-type tumor-associated macrophages infiltrate more in HER2-overexpressing gastric cancer tissues, suggesting that the HER2 signaling pathway may be involved in the construction of an immunosuppressive microenvironment [16, 17]. However, most of these studies only focus on the overall density of TILs or specific functional subgroups, ignoring the spatial distribution differences of TILs - that is, the heterogeneous distribution pattern of immune cells between the tumor center (CT) and the invasive margin (IM).

Recent studies have shown that the anti-tumor effect of immune cells not only depends on their absolute quantity, but also on their spatial position within the tumor and the depth of infiltration. In colorectal cancer, non-small cell lung cancer, and melanoma, researchers have found that a dense distribution of TILs at the invasive margin often indicates that immune cells are "excluded" from tumor nests, and this "edge-limiting" immune phenotype is significantly associated with poorer prognosis and low response rates to immunotherapy [18]. By calculating the ratio of edge/central TILs (E/C ratio), the ability of immune cells to penetrate from the edge to the center can be quantitatively measured, thereby more accurately depicting the degree of immune exclusion in the tumor [19]. However, in gastric adenocarcinoma, especially the spatial immune distribution pattern associated with HER2 expression status, there is still a lack of digital and quantitative systematic evaluation.

The popularization of whole slide imaging (WSI) technology and the development of open-source image analysis software (such as QuPath) have made it possible to conduct large-scale, standardized spatial quantitative assessment of TILs based on conventional H&E stained sections, without the need for additional immunohistochemical staining. This is feasible in the routine pathology department [20]. This digital retrospective assessment method has the advantages of low cost, strong repeatability, and ease of promotion, and is suitable for exploring and validating new pathological biomarkers in real-world research.

Based on the above background, this study intends to utilize digital pathology technology to conduct a retrospective analysis on a group of patients with resected gastric adenocarcinoma. The aim is: (1) To quantitatively compare the differences in CT-TILs, IM-TILs and E/C ratios between the HER2 positive and negative groups; (2) To analyze the correlation between spatial parameters of TILs and overall survival, and to evaluate their independent prognostic value; (3) To explore the distribution characteristics of E/C ratios in different pT stages and HER2 subgroups. We hypothesize that HER2-positive gastric adenocarcinoma tends to present an "edge-limited" immune phenotype with elevated E/C ratios, and this phenotype is an independent factor for poor prognosis. This work is expected to provide a retrospective evidence-based foundation for the precise immune stratification of HER2-positive gastric cancer and the optimization of targeted/immunotherapy combined treatment strategies.

Materials and methods

Research design and patients

This study was a single-center, retrospective case series study. It was approved by ethics committee of the First Affiliated Hospital of Lishui University, Lishui People's Hospital and

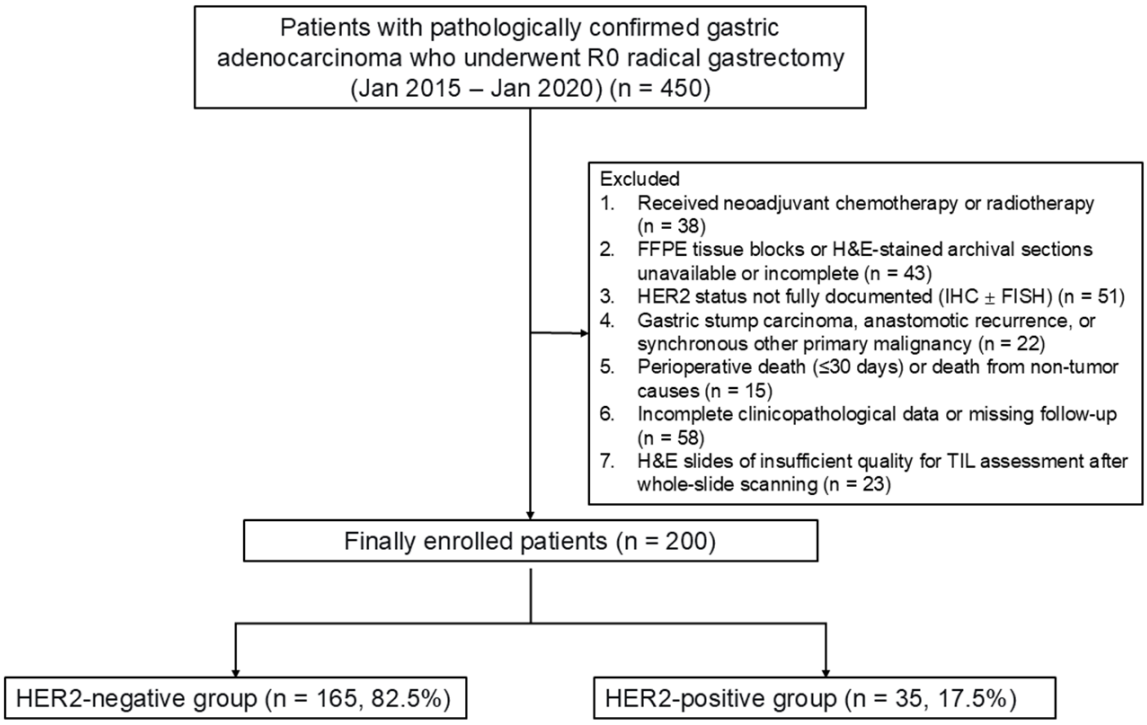

Figure 1. Flow chart of patient enrollment.

no informed consent was required. We continuously collected patients who underwent radical gastrectomy for gastric cancer in the general surgery department of the Lishui People's Hospital from January 2015 to January 2020, whose postoperative pathological diagnosis was gastric adenocarcinoma and whose archived tissue wax blocks were complete. All procedures performed in this study involving human participants were in accordance with the Declaration of Helsinki (as revised in 2013) (**Figure 1**).

Inclusion and exclusion criteria

The enrolled patients must have complete postoperative formalin-fixed paraffin-embedded (FFPE) tissue and corresponding hematoxylin-eosin (H&E) stained archived sections. They must not have received any neoadjuvant chemotherapy or radiotherapy before the surgery. Each patient must have a clearly archived HER2 immunohistochemistry (IHC) test result. For cases with an IHC score of 2+, there must also be concurrent or archived fluorescence in situ hybridization (FISH) test results to clarify the gene amplification status. Additionally, all the clinical and pathological data and postoperative follow-up records of the enrolled patients must be complete, and at least one standardized postoperative follow-up evaluation must have been completed.

Patients with any of the following conditions will be excluded: patients with residual gastric cancer, anastomotic recurrence cancer, or those with primary malignant tumors in other organs; patients who died during the perioperative period (within 30 days after surgery) or due to non-tumor-related causes; patients whose H&E stained sections after full slide scanning were evaluated by the pathologist as having severe fading, tissue folds, extensive necrosis, or slide damage, resulting in insufficient image quality for TILs readers; and patients with missing follow-up information or those who were lost to follow-up.

Clinical pathological data collection

The following indicators were extracted from the electronic medical record system and the pathological information system, and were independently entered by one researcher and verified by a second: (1) Demographic information: age, gender; (2) Lifestyle and past medical

history: smoking history (smoking, quit smoking, never), alcohol consumption history (frequent, occasional, never), body mass index (BMI, measured within one week before surgery), history of hypertension, diabetes, coronary heart disease, gastric cancer family history; (3) Preoperative laboratory tests: carcinoembryonic antigen (CEA, ng/mL); (4) Tumor characteristics: tumor location (cardia/gastric fundus, gastric body, gastric antrum), Bormann classification, Lauren classification, histological grade (high/middle/low differentiation); (5) Surgical information: surgical method (proximal gastrectomy, distal gastrectomy, total gastrectomy); (6) Postoperative pathology: pT stage, pN stage (based on the 8th edition of the AJCC gastric cancer TNM staging system), maximum tumor diameter (cm), vascular invasion (LVI, present/absent), nerve invasion (PNI, present/absent), postoperative adjuvant chemotherapy status (present/absent). All pathological diagnoses were the standard output of routine postoperative pathological reports and were not re-reviewed.

HER2 testing and interpretation

The HER2 status was directly taken from the standard pathological report issued by the clinic. The test was conducted using the IHC method (antibody: 4B5, Roche Ventana) and, when necessary, FISH (PathVysion HER2 DNA Probe Kit) was used for confirmation. According to the ASCO/CAP gastric cancer HER2 testing guidelines (2018 edition), an IHC score of 3+ was defined as HER2 positive, an IHC score of 0/1+ as HER2 negative; those with an IHC score of 2+ were further tested by FISH, with gene amplification (HER2/CEP17 ratio ≥ 2.0 or average HER2 copy number ≥ 6.0 signals/cell) classified as HER2 positive, and no amplification classified as negative. Based on this, patients were divided into the HER2 negative group and the HER2 positive group.

Digital pathology and assessment of TILs spatial distribution

All archived H&E stained sections of the enrolled cases were scanned using a full-slide scanner (such as 3DHISTECH Pannoramic MIDI, ×40 magnification, resolution 0.25 μm/pixel) as digital pathological images (svs format). Two pathologists who were unaware of the clinical prognosis independently completed the spatial quantitative assessment of TILs on the open-source software QuPath (v0.3.2). In case of inconsistencies, consensus was reached through negotiation.

According to the GI-TILs assessment method recommended by the International Immuno-Oncology Biomarker Working Group (IIOB), the density percentage of stromal TILs (sTILs) was emphasized. The specific steps are as follows:

Region selection and annotation: On each digital slide, avoid obvious necrosis, bleeding areas, and large blood vessels, and respectively define two fixed areas - (1) Tumor center (CT): located within the tumor substance, at least 1 mm away from the invasive edge (i.e., the junction between cancer and normal tissue); (2) Invasive edge (IM): defined as the junction between the cancer nests and the surrounding normal gastric wall tissue, with a band-like area extending approximately 500 μm on either side of the cancer-normal interface.

TILs counting: In the selected areas, at ×400 magnification, randomly select 3 to 5 high-power fields, visually assess the percentage of the area occupied by single-nucleus inflammatory cells (lymphocytes, plasma cells) in the stromal region (%). Exclude areas with dense neutrophils, eosinophilic granulocytes, and lymphoid follicle structures. Parameter recording: The densities (in %) of CT-TILs and IM-TILs were separately recorded, and the edge/center ratio (E/C ratio = IM-TILs/CT-TILs) was calculated. When CT-TILs was 0, the E/C ratio was set to a constant maximum value of 10. The optimal cut-off value for the E/C ratio was determined by maximizing the log-rank statistic, and patients were divided into high E/C (> cut-off) and low E/C (≤ cut-off) groups for survival analysis.

Each observer re-evaluated 10% (20 cases) of the randomly selected sections 4 weeks later. The consistency was evaluated using the intraclass correlation coefficient (ICC) and the interclass correlation coefficient. A coefficient of ICC > 0.8 was considered as good consistency. The intraclass correlation coefficient (ICC) for TILs assessment was 0.87 (95% CI: 0.79-0.93), indicating excellent inter-observer agreement. A schematic representation of these regions is provided in Supplementary Figure 1.

Follow-up and outcome indicators

Postoperative follow-up was conducted through outpatient visits, inpatient re-examinations, and telephone inquiries. The frequency of follow-up was once every 3-6 months in the first 2 years, once every 6-12 months in the third to fifth years, and once a year thereafter. The follow-up content included physical examination, tumor markers, endoscopy, and imaging examinations. The definition of outcome indicators is as follows: (1) Overall survival (OS): from the date of surgery to death due to any cause or the date of the last follow-up; (2) Disease-free survival (DFS): from the date of surgery to the date of the first pathological or imaging-confirmed recurrence/metastasis or death due to any cause, whichever occurs first. The last follow-up date was December 31, 2024, with a median follow-up time of 25 months.

Statistical analysis

Statistical analysis was performed using SPSS 20.0 and Python (v3.8). Continuous variables were tested for normality, and non-normally distributed continuous variables were summarized as median (interquartile range) or mean ± standard deviation. Group comparisons were performed using the Mann-Whitney U test; categorical variables were expressed as frequency (percentage), and group comparisons were conducted using the χ^2 test or Fisher's exact test. Correlation analysis between HER2 status and spatial parameters of TILs was performed using Spearman rank correlation. Survival analysis was plotted using the Kaplan-Meier method, and group comparisons were performed using the log-rank test; median survival time and its 95% confidence interval were provided. Univariate and multivariate analyses were conducted using the Cox proportional hazards regression model, with variables from the univariate analysis that had a *P* value < 0.10 and those with important clinical value included in the multivariate model. Results were expressed as risk ratio (HR) and 95% confidence interval (CI). All tests were two-sided, and a *P* value < 0.05 was considered statistically significant. Percentages were rounded to one decimal place, and other statistics were rounded to three decimal places.

Results

Patient baseline characteristics

A total of 200 patients with gastric adenocarcinoma who underwent radical resection were included in this study. Among them, 165 cases (82.5%) were in the HER2-negative group and 35 cases (17.5%) were in the HER2-positive group. There were no statistically significant differences in age, gender, BMI, smoking history, drinking history, tumor location, Bormann classification, Lauren classification, histological grade, surgical method, pT stage, pN stage, vascular invasion, nerve invasion, and the proportion of postoperative adjuvant chemotherapy between the two groups (P > 0.05), indicating that baseline characteristics were well balanced between the two groups. It is notable that the proportion of diabetic patients in the HER2-positive group was significantly higher than that in the negative group (22.9% vs. 7.9%, P = 0.015), while there were no significant differences in other comorbidities (hypertension, coronary heart disease) and family history of gastric cancer. The detailed comparison of baseline clinical and pathological characteristics is shown in **Table 1**.

Correlation between the spatial distribution pattern of TILs and HER2 expression status

We quantitatively evaluated the percentage of interstitial TILs density in the tumor center (CT) and the invasive margin (IM) using digital pathological images, and calculated the edge/center ratio (E/C ratio). The mean ± standard deviation of CT-TILs, IM-TILs, and E/C ratio in the entire group were 19.39% ± 11.50%, 23.32% ± 13.38%, and 1.40 ± 1.08, respectively.

Stratified analysis by HER2 status showed that the CT-TILs density in the HER2-positive group was significantly lower than that in the negative group (11.92% ± 8.47% vs. 20.98% ± 11.45%, Mann-Whitney U = 4271.000, P < 0.001), while there was no significant difference in IM-TILs density between the two groups (22.31% ± 15.14% vs. 23.54% ± 13.02%, U = 3170.000, P = 0.365). This led to a significantly higher E/C ratio in the HER2-positive group than in the negative group (2.11 ± 1.04 vs. 1.25 ± 1.03, U

Table 1. Baseline clinicopathological characteristics of the patients compared by HER2 status

Variable	HER2 Negative (n = 165)	HER2 Positive (n = 35)	U/χ^2	*P*-value
Age	59.35 ± 9.52	57.66 ± 8.01	3215.500	0.292
BMI	23.66 ± 3.06	23.57 ± 3.14	2954.500	0.831
CEA	4.67 ± 4.02	4.06 ± 2.78	3046.000	0.611
Max_diameter	5.47 ± 2.38	4.94 ± 2.05	3275.000	0.213
Sex			0.901	0.342
Male	111 (67.3%)	20 (57.1%)	-	-
Female	54 (32.7%)	15 (42.9%)	-	-
Smoking			0.002	0.968
Smoker	52 (31.5%)	12 (34.3%)	-	-
Ex-smoker	0 (0.0%)	0 (0.0%)	-	-
Never	91 (55.2%)	19 (54.3%)	-	-
Alcohol drinking			1.036	0.596
Often	10 (6.1%)	1 (2.9%)	-	-
Occasionally	55 (33.3%)	10 (28.6%)	-	-
Never	100 (60.6%)	24 (68.6%)	-	-
HTN			0.290	0.590
Yes	48 (29.1%)	8 (22.9%)	-	-
No	117 (70.9%)	27 (77.1%)	-	-
DM			Fisher	0.015
Yes	13 (7.9%)	8 (22.9%)	-	-
No	152 (92.1%)	27 (77.1%)	-	-
CAD			Fisher	0.704
Yes	10 (6.1%)	3 (8.6%)	-	-
No	155 (93.9%)	32 (91.4%)	-	-
Family_history			Fisher	0.379
Yes	20 (12.1%)	2 (5.7%)		
No	145 (87.9%)	33 (94.3%)	-	-
Tumor_site			0.284	0.868
Cardia/Fundus	34 (20.6%)	7 (20.0%)	-	-
Body	49 (29.7%)	9 (25.7%)	-	-
Antrum	82 (49.7%)	19 (54.3%)	-	-
Bormann			3.007	0.391
Borrmann I	8 (4.8%)	1 (2.9%)	-	-
Borrmann II	50 (30.3%)	8 (22.9%)	-	-
Borrmann III	83 (50.3%)	17 (48.6%)	-	-
Borrmann IV	24 (14.5%)	9 (25.7%)	-	-
Lauren			3.585	0.167
Intestinal	84 (50.9%)	22 (62.9%)	-	-
Diffuse	51 (30.9%)	11 (31.4%)	-	-
Mixed	30 (18.2%)	2 (5.7%)	-	-
Grade			0.766	0.682
Well differentiated	11 (6.7%)	1 (2.9%)	-	-
Moderately differentiated	61 (37.0%)	13 (37.1%)	-	-
Poorly differentiated	93 (56.4%)	21 (60.0%)	-	-
Surgery_type			0.295	0.863
Proximal gastrectomy	23 (13.9%)	4 (11.4%)		
Distal gastrectomy	83 (50.3%)	17 (48.6%)	-	-
Total gastrectomy	59 (35.8%)	14 (40.0%)	-	-

pT			2.932	0.402
pT1	14 (8.5%)	3 (8.6%)	-	-
pT2	34 (20.6%)	11 (31.4%)	-	-
pT3	75 (45.5%)	11 (31.4%)	-	-
pT4	42 (25.5%)	10 (28.6%)	-	-
pN			0.645	0.886
pN0	48 (29.1%)	12 (34.3%)	-	-
pN1	33 (20.0%)	6 (17.1%)	-	-
pN2	45 (27.3%)	8 (22.9%)	-	-
pN3	39 (23.6%)	9 (25.7%)	-	-
LVI			0.176	0.675
Yes	80 (48.5%)	15 (42.9%)	-	-
No	85 (51.5%)	20 (57.1%)	-	-
PNI			0.243	0.622
Yes	62 (37.6%)	11 (31.4%)	-	-
No	103 (62.4%)	24 (68.6%)	-	-
Adjuvant_chemo			0.837	0.360
Yes	128 (77.6%)	24 (68.6%)	-	
No	37 (22.4%)	11 (31.4%)	-	-

Note: Continuous variables are expressed as mean ± standard deviation; group differences assessed by Mann-Whitney U test. Categorical variables are expressed as n (%). Group comparisons used Chi-square test or Fisher's exact test when expected cell frequency < 5. For categorical variables, 'Statistic' column shows Chi-square value; 'Fisher' indicates Fisher's exact test was applied. *P* values are two-sided and considered statistically significant at P < 0.05. Abbreviation: HER2, human epidermal growth factor receptor 2; BMI, body mass index; CEA, carcinoembryonic antigen; HTN, hypertension; DM, diabetes mellitus; CAD, coronary artery disease; LVI, lymphovascular invasion; PNI, perineural invasion; pT, pathological tumor stage; pN, pathological nodal stage.

Table 2. Correlation analysis of tumor-infiltrating lymphocyte spatial parameters and HER2 status

Variable	Total (n = 200)	HER2 Negative (n = 165)	HER2 Positive (n = 35)	Statistic	P_U	Spearman_rho	P_rho
CT_TILs	19.39 ± 11.50	20.98 ± 11.45	11.92 ± 8.47	4271.000	0.000	-0.315	< 0.001
IM_TILs	23.32 ± 13.38	23.54 ± 13.02	22.31 ± 15.14	3170.000	0.365	-0.064	0.365
E_C_ratio	1.40 ± 1.08	1.25 ± 1.03	2.11 ± 1.04	728.000	0.000	0.492	< 0.001
CD8_pct	11.11 ± 7.46	12.48 ± 7.37	4.67 ± 3.49	4793.500	0.000	-0.434	< 0.001
FOXP3_pct	3.85 ± 3.56	3.26 ± 3.16	6.61 ± 4.07	1171.500	0.000	0.391	< 0.001
CD8_FOXP3_ratio	6.92 ± 11.60	8.05 ± 12.42	1.55 ± 2.76	4956.500	0.000	-0.472	< 0.001

Note: Bonferroni correction for three comparisons set the significance threshold at P < 0.017. Abbreviation: CT-TILs, center of tumor stromal TILs; IM-TILs, invasive margin stromal TILs; E/C ratio, edge/center ratio; HER2, human epidermal growth factor receptor 2.

= 728.000, P < 0.001) (**Table 2**; **Figure 2A-C**). Spearman correlation analysis further confirmed that HER2 status (binary variable) was negatively correlated with CT-TILs (ρ = -0.315, P < 0.001) and positively correlated with E/C ratio (ρ = 0.492, P < 0.001), but there was no significant correlation with IM-TILs (ρ = -0.064, P = 0.365) (**Table 2**).

Scatter plots visually demonstrate the relationship between the E/C ratio and CT-TILs and IM-TILs: the E/C ratio decreased as CT-TILs increased, and there was no significant linear trend with IM-TILs, and HER2-positive cases were mainly distributed in the areas with lower CT-TILs and higher E/C ratio (**Figure 3A**, **3B**). This spatial distribution feature suggested that HER2-positive gastric cancer tended to present an "edge-limiting" immune phenotype, that is, immune cells aggregated at the invasive margin and were difficult to penetrate the tumor center.

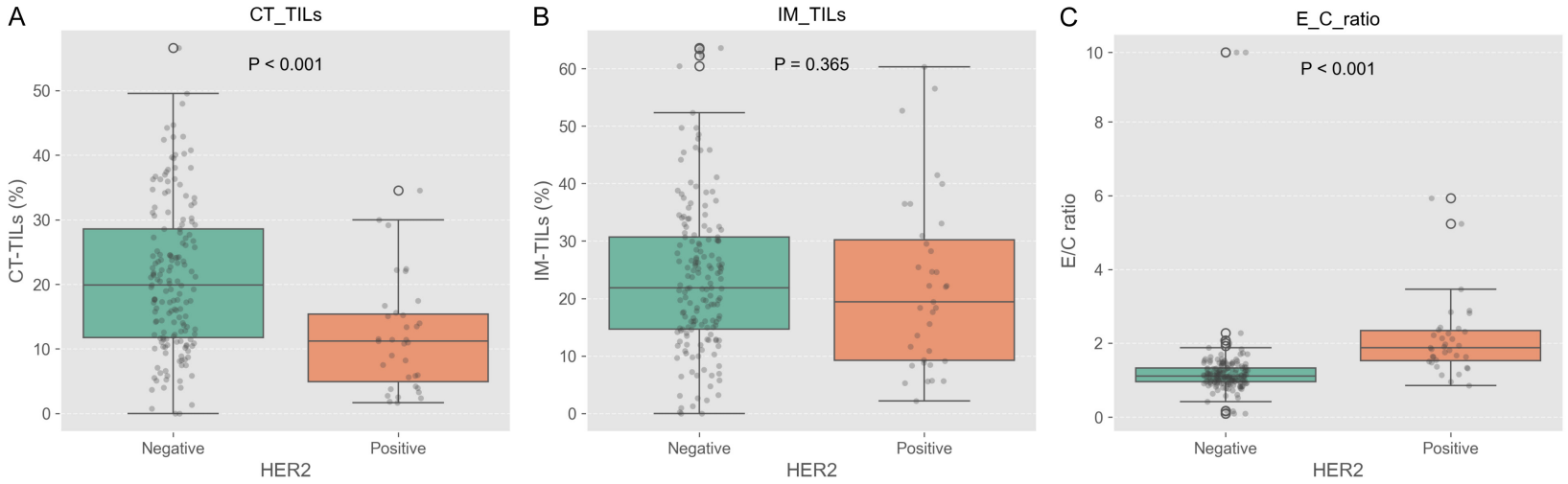

Figure 2. Comparison of tumor-infiltrating lymphocyte spatial parameters between HER2-negative and HER2-positive groups. A. CT-TILs (center of tumor stromal TILs, %). The HER2-positive group had significantly lower CT-TILs than the HER2-negative group (P < 0.001, Mann-Whitney U test). B. IM-TILs (invasive margin stromal TILs, %). No significant difference was observed (P = 0.365). C. E/C ratio (IM-TILs/CT-TILs). The HER2-positive group had a significantly higher E/C ratio (P < 0.001). Boxplots show median, interquartile range, and whiskers extending to 1.5× the interquartile range; overlaid dots represent individual cases. *P* values are displayed in each panel. Abbreviation: CT-TILs, center of tumor stromal TILs; IM-TILs, invasive margin stromal TILs; E/C ratio, edge/center ratio (IM-TILs/CT-TILs); HER2, human epidermal growth factor receptor 2.

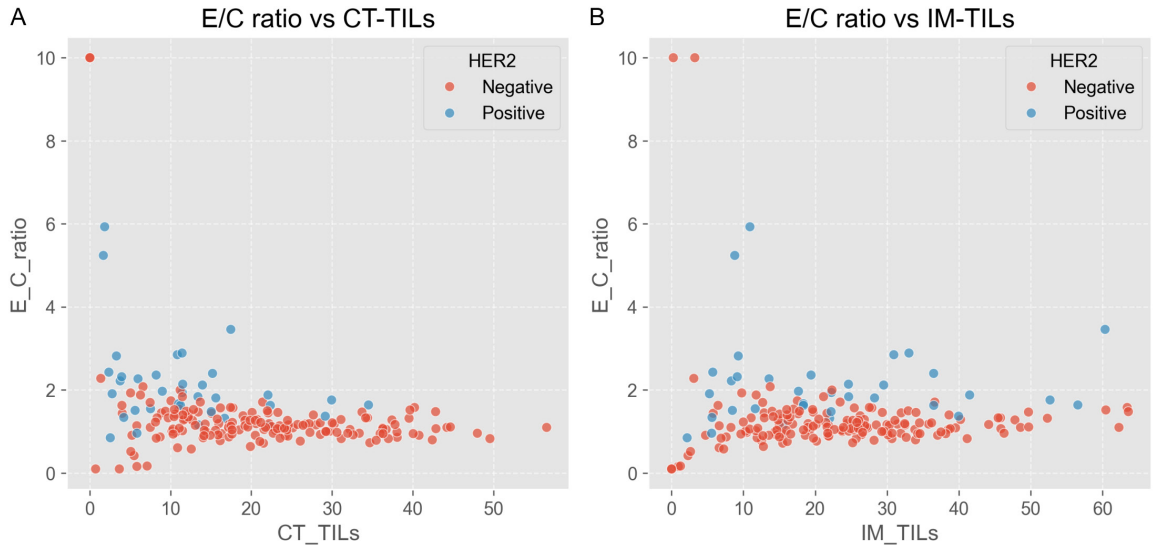

Figure 3. Scatter plots of the E/C ratio versus CT-TILs and IM-TILs. A. E/C ratio versus CT-TILs. Higher E/C ratios were predominantly observed in tumors with low CT-TILs, particularly in the HER2-positive group. B. E/C ratio versus IM-TILs. No clear linear trend was evident between E/C ratio and IM-TILs. HER2-positive cases clustered in the region of low CT-TILs and high E/C ratio, consistent with an immune-excluded phenotype. Abbreviation: CT-TILs, center of tumor stromal TILs; IM-TILs, invasive margin stromal TILs; E/C ratio, edge/center ratio; HER2, human epidermal growth factor receptor 2.

Lymphocyte subset analysis by immunohistochemistry and stratified ROC validation

To further characterize the immune microenvironment, we assessed $CD8^+$ cytotoxic T-cell and $FOXP3^+$ regulatory T-cell (Treg) densities by immunohistochemistry. As shown in **Table 2** and Supplementary Figure 2, HER2-positive tumors exhibited significantly lower $CD8^+$ T-cell density (mean ± SD: 4.67% ± 3.49% vs. 12.48% ± 7.37%; Mann-Whitney U = 4793.5, P < 0.001) and significantly higher $FOXP3^+$ Treg density (6.61% ± 4.07% vs. 3.26% ± 3.16%; U = 1171.5, P < 0.001) compared with HER2-negative tumors. Consequently, the CD8/FOXP3 ratio was markedly reduced in the HER2-positive group (1.55 ± 2.76 vs. 8.05 ± 12.42; U = 4956.5, P < 0.001).

Spearman correlation analysis revealed that the E/C ratio was negatively correlated with $CD8^+$ density (ρ = -0.371, P < 0.001) and positively correlated with $FOXP3^+$ density (ρ = 0.467, P < 0.001). The CD8/FOXP3 ratio showed a strong negative correlation with the E/C ratio in the whole cohort (ρ = -0.484, P < 0.001) and remained significant in the HER2-positive subgroup (ρ = -0.470, P = 0.004) (Supplementary Figure 3).

To validate the stability of the HER2-E/C interaction, we performed time-dependent ROC analysis stratified by HER2 status. As shown in Supplementary Figure 4, the E/C ratio predicted 12-month and 36-month overall survival with area under the curve (AUC) values of 0.864 and 0.859, respectively, in the HER2-positive subgroup, whereas the AUCs in the HER2-negative subgroup were only 0.490 and 0.571. These results confirm that the prognostic value of the E/C ratio is largely confined to HER2-positive patients.

The relationship between TILs spatial parameters and prognosis

The optimal cut-off value for the E/C ratio, determined by maximizing the log-rank statistic, was 1.57. Using this cut-off, patients were divided into high E/C (E/C > 1.57) and low E/C (E/C ≤ 1.57) groups. In the entire cohort, the high E/C group had significantly worse overall survival (OS) than the low E/C group (median OS: 14.64 months vs. 42.87 months; log-rank statistic = 17.712, P < 0.001) (**Figure 4**).

Subgroup analysis by HER2 status revealed that in the HER2-negative subgroup, there was no significant difference in OS between high

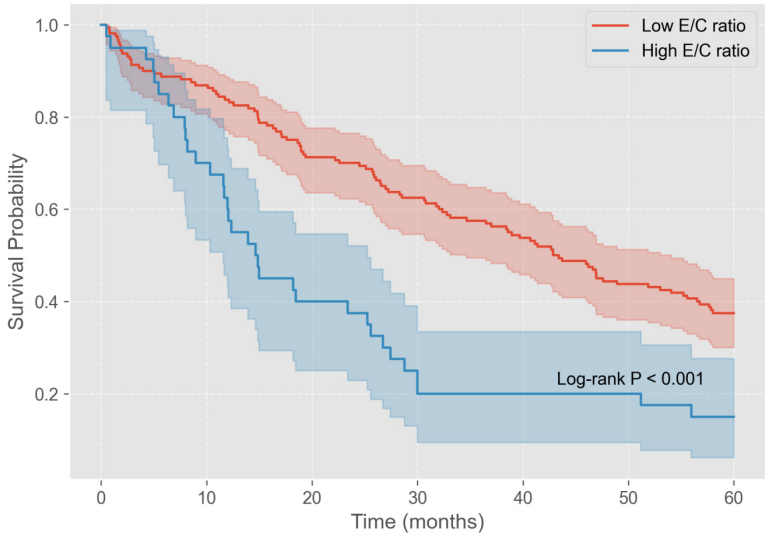

Figure 4. Kaplan-Meier curves for overall survival according to the E/C ratio in the entire cohort (optimal cut-off = 1.57). The high E/C group (E/C > 1.57, n = 40) had significantly worse overall survival than the low E/C group (E/C ≤ 1.57, n = 160) with median OS of 14.64 months vs. 42.87 months (log-rank statistic = 17.712, P < 0.001). Univariate Cox regression gave a hazard ratio of 2.281 (95% CI: 1.537-3.384) for high vs. low E/C. Abbreviation: E/C ratio, edge/center ratio; OS, overall survival.

and low E/C groups (median OS: 14.98 vs. 43.40 months; log-rank statistic = 3.163, P = 0.075). In the HER2-positive subgroup, the high E/C group had significantly shorter OS compared to the low E/C group (median OS: 12.34 vs. 32.78 months; log-rank statistic = 4.994, P = 0.025) (**Figure 5**; **Table 3**).

Multivariate Cox regression analysis

Multivariate Cox regression analysis was performed adjusting for age, sex, smoking, pT stage, pN stage, LVI, PNI, adjuvant chemotherapy, HER2 status, DM, and CEA. The results showed that pT stage (HR = 1.721, 95% CI 1.115-2.657, P = 0.014), pN stage (HR = 3.106, 95% CI 2.065-4.670, P < 0.001), LVI (HR = 1.827, 95% CI 1.250-2.670, P = 0.002) remained independent prognostic factors for OS, while PNI was not significant (HR = 1.156, 95% CI 0.795-1.682, P = 0.447). The E/C ratio as a continuous variable was independently associated with OS (HR = 1.398, 95% CI 1.171-1.669, P < 0.001). Moreover, a significant interaction between HER2 status and E/C ratio was observed (HR = 1.844, 95% CI 1.273-2.670, P = 0.001), suggesting that the prognostic impact of E/C ratio is modified by HER2 expression (**Table 4**; **Figure 6**).

Correlation between spatial parameters of TILs and clinical pathological characteristics

The Spearman correlation matrix heatmap showed that CT-TILs were highly positively correlated with IM-TILs (ρ = 0.886), while the E/C ratio was moderately negatively correlated with CT-TILs (ρ = -0.331) and weakly correlated with IM-TILs (ρ = 0.069) (**Figure 7**). Moreover, the E/C ratio was weakly negatively correlated with the maximum tumor diameter (ρ = -0.166), that is, the E/C ratio tended to decrease with increasing tumor size. Indicators such as age, BMI, preoperative CEA, etc. had no significant correlation with the parameters of TILs (|ρ| < 0.1), suggesting that spatial immune characteristics are not affected by common confounding factors. Further analysis of the distribution of the E/C ratio in different pT stages and HER2 statuses (**Figure 8**) revealed that as the pT stage increased, the E/C ratio generally showed a downward trend. In the pT1-T3 stages, the E/C ratio of the HER2-positive group was higher than that of the negative group, especially in the pT2 stage, where the difference was most significant. In the pT4 stage, the two groups tended to be similar. This phenomenon suggests that the immune exclusion characteristics related to HER2 may be more prominent in the earlier stages of the tumor (pT2-T3), and when the tumor progresses to the locally advanced stage, the differences in spatial immune patterns may be weakened by other immune escape mechanisms.

Discussion

This study retrospectively analyzed the spatial distribution patterns of tumor-infiltrating lymphocytes (TILs) in 200 patients who underwent radical resection for gastric adenocarcinoma using digital pathological images. It is the first to systematically report the correlations between tumor center (CT) TILs, infiltrating

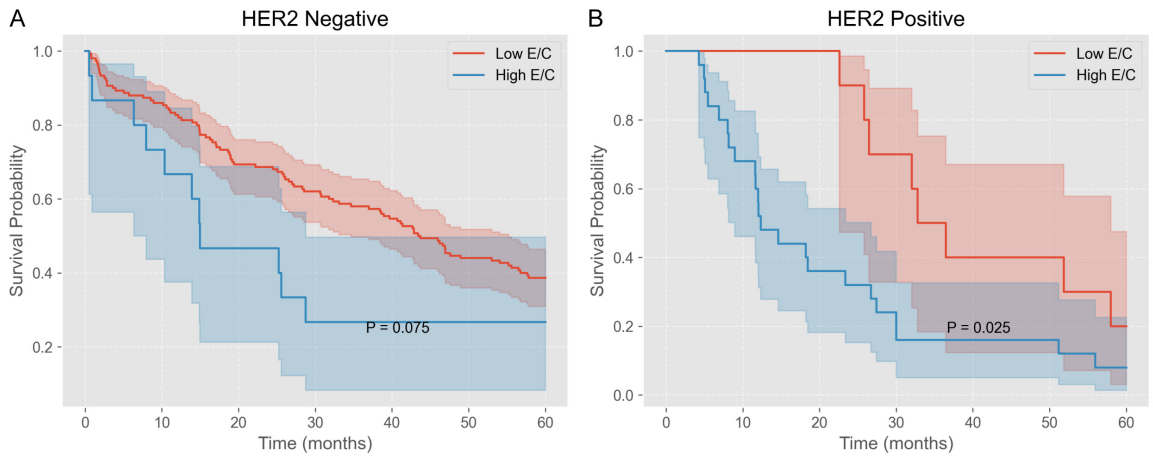

Figure 5. Kaplan-Meier curves for overall survival stratified by the E/C ratio in HER2-negative and HER2-positive subgroups. A. HER2-negative subgroup. The low-E/C (E/C ≤ 1.57, n = 150) and high-E/C (E/C > 1.57, n = 15) groups did not differ significantly in overall survival (median OS: 43.40 vs. 14.98 months; log-rank statistic = 3.163, P = 0.075). B. HER2-positive subgroup. The high-E/C group (n = 25) had significantly shorter overall survival than the low-E/C group (n = 10) (median OS: 12.34 vs. 32.78 months; log-rank statistic = 4.994, P = 0.025). Hazard ratios (univariate Cox) were 1.755 (95% CI: 0.937-3.287) for HER2-negative and 2.479 (95% CI: 1.095-5.615) for HER2-positive patients. Hazard ratios and 95% confidence intervals are derived from univariate Cox regression. Abbreviation: E/C ratio, edge/center ratio; OS, overall survival; HER2, human epidermal growth factor receptor 2.

Table 3. Comparison of median overall survival stratified by E/C ratio in HER2-negative and HER2-positive subgroups

HER2 Status	Median OS Low E/C	Median OS High E/C	Statistic	*P*-value
Negative	43.40	14.98	3.163	0.075
Positive	32.78	12.34	4.994	0.025

Note: Abbreviation: E/C ratio, edge/center ratio; OS, overall survival; HER2, human epidermal growth factor receptor 2.

margin (IM) TILs, and the edge/center ratio (E/C ratio) with HER2 expression status and their prognostic value. The main findings can be summarized as follows: First, HER2-positive gastric adenocarcinoma presents a typical "margin-limiting" immune phenotype, with significantly reduced CT-TILs density and significantly increased E/C ratio; Second, the E/C ratio as a continuous variable was independently associated with OS after full adjustment (HR = 1.398, P < 0.001), and dichotomization at an optimal cut-off of 1.57 also provided significant prognostic stratification (log-rank P < 0.001). Third, a significant interaction between HER2 status and E/C ratio was observed (HR = 1.844, P = 0.001), indicating that the prognostic impact of E/C ratio differs by HER2 expression. These findings add a new spatial dimension to the understanding of the heterogeneity of the tumor microenvironment in gastric adenocarcinoma and provide a feasible path for clinical translation based on conventional pathological sections for immune phenotype stratification.

The involvement of the HER2 signaling pathway in the formation of the immune exclusion microenvironment has been confirmed by numerous experimental studies. In preclinical models of breast cancer and gastric cancer, HER2 overexpression activates the PI3K/AKT/mTOR pathway, upregulating secreted factors such as vascular endothelial growth factor (VEGF) and interleukin-6, and simultaneously inhibits STING pathway-dependent type I interferon production, thereby hindering the activation of dendritic cells and the effective recruitment of $CD8^+$ T cells to the tumor [21, 22]. Moreover, HER2-positive tumors often present a disrupted chemokine spectrum, such as the downregulation of Th1-type chemokines like CXCL9 and CXCL10, which weakens the ability of effector T cells to self-infiltrate from the periphery along the chemokine gradient

Table 4. Univariate and multivariate Cox regression analysis for overall survival in gastric adenocarcinoma

Variable	HR (Uni)	95% CI (Uni)	P (Uni)	HR (Multi)	95% CI (Multi)	P (Multi)
Age	1.001	0.982-1.021	0.908	0.999	0.979-1.019	0.900
Sex_bin	1.395	0.964-2.021	0.078	1.445	0.949-2.199	0.086
Smoking_bin	1.509	1.063-2.143	0.021	1.201	0.805-1.793	0.369
Drinking_bin	0.477	0.195-1.165	0.104	-	-	-
BMI	1.021	0.967-1.079	0.453	-	-	-
HTN_bin	0.832	0.564-1.228	0.354	-	-	-
DM_bin	1.339	0.794-2.258	0.274	1.015	0.571-1.807	0.958
CAD_bin	1.357	0.712-2.586	0.354	-	-	-
Family_bin	1.373	0.844-2.233	0.202	-	-	-
CEA	0.995	0.953-1.039	0.811	1.016	0.971-1.062	0.500
pT_num	1.654	1.136-2.407	0.009	1.721	1.115-2.657	0.014
pN_num	2.382	1.629-3.482	< 0.001	3.106	2.065-4.670	< 0.001
Max_diameter	1.068	0.992-1.149	0.080	-	-	-
LVI_bin	1.674	1.191-2.353	0.003	1.827	1.250-2.670	0.002
PNI_bin	1.139	0.804-1.615	0.463	1.156	0.795-1.682	0.447
Adjuvant_bin	0.843	0.575-1.237	0.383	0.672	0.437-1.032	0.069
HER2_bin	1.953	1.303-2.929	0.001	0.415	0.176-0.975	0.044
CT_TILs	0.978	0.963-0.994	0.006	-	-	-
IM_TILs	0.994	0.981-1.007	0.346	-	-	-
E_C_ratio	1.483	1.312-1.676	< 0.001	1.398	1.171-1.669	< 0.001
HER2_E_C_inter	-	-	-	1.844	1.273-2.670	0.001

Note: Abbreviation: OS, overall survival; HR, hazard ratio; CI, confidence interval; HER2, human epidermal growth factor receptor 2; LVI, lymphovascular invasion; PNI, perineural invasion; DM, diabetes mellitus; CEA, carcinoembryonic antigen; pT, pathological tumor stage; pN, pathological nodal stage.

towards the tumor's deep layers, ultimately resulting in a "rejection-like" microenvironment with a lack of immune cells in the central region [23, 24]. In this study, the density of CT-TILs in the HER2-positive group showed a selective decrease, while the density of IM-TILs did not show significant differences. This is highly consistent with the above mechanism hypothesis. In contrast, in the HER2-negative group, CT-TILs were relatively high, and the E/C ratio was close to 1, suggesting that most of these tumors may have immune "infiltration" characteristics, and some cases may be associated with a higher tumor mutation burden (TMB) or microsatellite instability (MSI-H) subtypes - this awaits further confirmation through subsequent multi-omics studies.

The E/C ratio as a continuous variable was independently associated with OS (HR = 1.398, P < 0.001), and the use of an optimal cut-off value (1.57) also successfully stratified patients into distinct prognostic groups in the overall cohort (log-rank P = 0.001). This suggests that the E/C ratio may have a threshold effect on survival rather than a linear dose-response relationship. Furthermore, the significant interaction between HER2 status and E/C ratio (P = 0.001) indicates that the prognostic value of E/C ratio is more pronounced in HER2-positive patients. In colorectal cancer, Galon et al. [25] established an immune scoring system that quantified the density of $CD3^+$ and $CD8^+$ T cells in the tumor center and the infiltrating margin, achieving high-precision stratification of the risk of recurrence, and its predictive efficacy was superior to the traditional TNM staging. In non-small cell lung cancer, multiple studies have confirmed that the "immune exclusion type" tumors, with $CD8^+$ T cells aggregating at the infiltration margin and absent in the central area, have a significantly lower response rate to PD-1/PD-L1 inhibitor monotherapy than the "immune inflammation type" tumors with high infiltration throughout the entire tumor [26]. However, it is worth noting that most of these

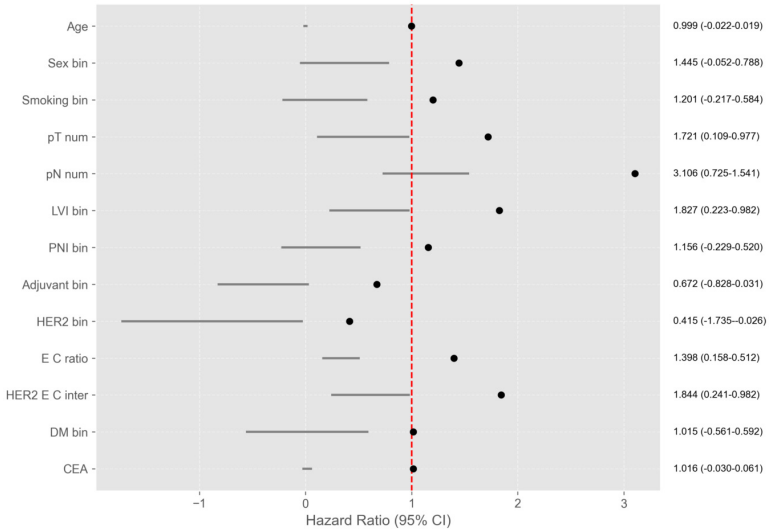

Figure 6. Forest plot of the multivariate Cox proportional hazards regression model. The model was adjusted for age, sex, smoking, pT stage, pN stage, LVI, PNI, adjuvant chemotherapy, HER2 status, DM, and CEA. The E/C ratio as a continuous variable was independently associated with OS (HR = 1.398, 95% CI: 1.171-1.669, P < 0.001), and the interaction term between HER2 status and E/C ratio was significant (HR = 1.844, 95% CI: 1.273-2.670, P = 0.001). Abbreviation: HR, hazard ratio; CI, confidence interval; OS, overall survival; HER2, human epidermal growth factor receptor 2; LVI, lymphovascular invasion; PNI, perineural invasion; DM, diabetes mellitus; CEA, carcinoembryonic antigen; pT, pathological tumor stage; pN, pathological nodal stage.

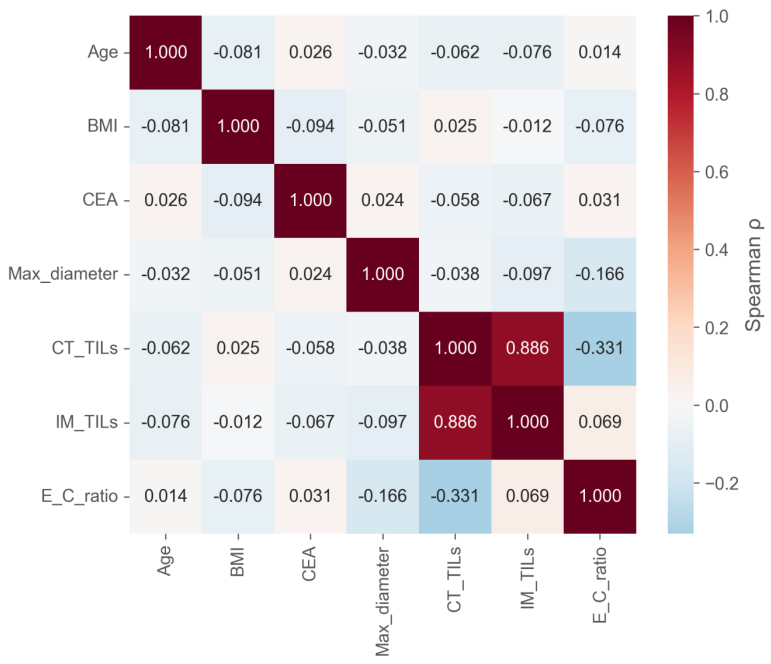

Figure 7. Heatmap of the Spearman correlation matrix between continuous clinical variables and TILs spatial parameters. Abbreviation: BMI, body mass index; CEA, carcinoembryonic antigen; CT-TILs, center of tumor stromal TILs; IM-TILs, invasive margin stromal TILs; E/C ratio, edge/center ratio.

studies relied on multiple immunohistochemical or immunofluorescence techniques, which were complex to operate and costly, limiting their application in routine pathology departments. This study was based on conventional H&E stained sections and used the open-source software QuPath to perform semi-quantitative assessment of the spatial distribution of TILs. The method was simple and cost extremely low, conforming to the practical operability of real-world retrospective studies. At the same time, pT stage, pN stage, vascular invasion, and nerve invasion were all significant survival predictors in univariate and multivariate Cox regression, consistent with the traditional understanding of gastric cancer prognosis research [27], which indirectly verified the reliability of this analysis process. The recent KEYNOTE-811 trial demonstrated that adding pembrolizumab to trastuzumab and chemotherapy significantly improves outcomes in HER2-positive advanced gastric cancer [28]. Although our study was not designed to assess immunotherapy response, the elevated E/C ratio in HER2-positive tumors may identify a subset with immune exclusion that could benefit from such combination strategies.

The interaction term between HER2 status and E/C ratio was statistically significant (HR = 1.844, 95% CI 1.273-2.670, P = 0.001), indicating that the effect of E/C ratio on OS differs by HER2 status. In HER2-positive patients, a

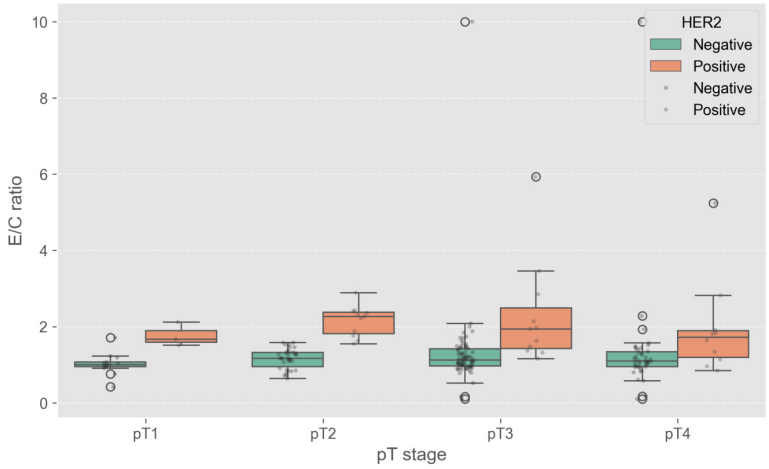

Figure 8. Distribution of the E/C ratio according to pT stage and HER2 status. Boxplots show medians, interquartile ranges, and individual data points. Mean ± SD values are: pT1: HER2-negative 1.02 ± 0.28 (n = 14), HER2-positive 1.77 ± 0.32 (n = 3); pT2: HER2-negative 1.16 ± 0.26 (n = 34), HER2-positive 2.16 ± 0.40 (n = 11); pT3: HER2-negative 1.29 ± 1.08 (n = 75), HER2-positive 2.30 ± 1.39 (n = 11); pT4: HER2-negative 1.33 ± 1.42 (n = 42), HER2-positive 1.96 ± 1.29 (n = 10). A downward trend of E/C ratio with increasing pT stage was observed, with HER2-positive tumors having higher E/C ratios in early stages (pT1-pT3). Abbreviation: E/C ratio, edge/center ratio; HER2, human epidermal growth factor receptor 2; pT, pathological tumor stage.

high E/C ratio was associated with a shorter median OS (12.34 vs. 32.78 months), consistent with the "immune-excluded" phenotype conferring a worse prognosis. This finding supports the hypothesis that HER2-positive gastric cancers with a high E/C ratio may represent a distinct immune microenvironment subtype that could benefit from combination strategies targeting both HER2 and immune exclusion. This trend is consistent with the exploratory research results of anti-HER2 combined immunotherapy in recent years. For example, the KEYNOTE-811 study showed that pembrolizumab combined with trastuzumab and chemotherapy could significantly improve the objective response rate in HER2-positive advanced gastric cancer, especially in the subgroups with higher PD-L1 combined positive score (CPS) or relatively abundant TILs [27]. The "edge-limiting" immune phenotype identified in this study may precisely define an intermediate immune state where immune cells have been mobilized to the tumor edge but have not effectively infiltrated. Such patients are most likely to achieve breakthrough efficacy from treatment strategies that eliminate immune exclusion, such as anti-VEGF drugs, CCR5 inhibitors combined with immune checkpoint inhibitors. Therefore, it is recommended that subsequent prospective studies incorporate E/C ratio or spatial immune phenotypes as preset biomarker stratification factors to verify their predictive value for the efficacy of targeted immunotherapy combinations.

The IHC data provide a functional correlate for the spatial E/C ratio pattern. The significantly lower $CD8^+$ T-cell density and higher $FOXP3^+$ Treg density in HER2-positive tumors align with the immune-excluded phenotype, where cytotoxic cells are kept at the tumor edge while regulatory cells accumulate. The strong inverse correlation between the CD8/FOXP3 ratio and the E/C ratio ($\rho = -0.484$, $P < 0.001$) supports the use of the E/C ratio as a surrogate marker for an immunosuppressive microenvironment, although formal validation with multiplex IHC or spatial transcriptomics is warranted.

Another notable finding of this study is that the E/C ratio shows an overall downward trend as the pT stage increases. In the pT1-T3 stages, the E/C ratio of the HER2-positive group is significantly higher than that of the negative group, while in the pT4 stage, the two groups gradually converge. This phenomenon suggests that the HER2-related immune exclusion characteristics may have formed and dominated the immune spatial pattern at an earlier stage of the tumor, but when the tumor progresses to locally advanced stage, extensive interstitial remodeling, the formation of physical barriers, and the release of widespread immunosuppressive factors (such as transforming growth factor-β, interleukin-10) may become stronger negative immune regulatory factors, thereby partially weakening the spatial immune effect of the HER2 signal itself [29-31]. This finding has practical guiding significance for the application of spatial immune parameters in clinical decision-making: if the E/C ratio is used as an auxiliary tool for prognosis stratification or treatment decision-making, the influence of

tumor stage should be fully considered, or at least independent stratification analysis should be conducted within the TNM classification.

Based on the optimal cut-off value of 1.57 identified in this study, we propose a practical workflow for implementing the E/C ratio in routine pathology practice. On standard H&E-stained sections, pathologists can use the QuPath platform (or any digital slide viewer with annotation tools) to delineate the tumor center (CT), defined as the area at least 1 mm away from the invasive margin, and the invasive margin (IM), defined as a 500 μm band centered on the cancer-normal interface. Stromal TIL densities (in percentage) in each region are visually estimated (or semi-quantified), and the E/C ratio is calculated as IM-TILs divided by CT-TILs. An E/C ratio greater than 1.57 indicates an "immune-excluded" phenotype. In a diagnostic report, the wording could be: "TIL spatial assessment: E/C ratio high (> 1.57), consistent with an immune-excluded pattern associated with worse overall survival". For HER2-positive gastric adenocarcinoma, a high E/C ratio may identify patients who are more likely to benefit from anti-HER2 therapy combined with immune-checkpoint inhibitors or agents that reverse immune exclusion (e.g., anti-VEGF or CCR5 inhibitors), although this hypothesis requires prospective validation. We therefore encourage future clinical trials to incorporate the E/C ratio as a stratification biomarker.

To address the lack of external validation, we have designed a multi-center retrospective study involving the First Affiliated Hospital of Wenzhou Medical University and Ningbo First Hospital. An independent cohort of approximately 120 patients with gastric adenocarcinoma (including at least 40 HER2-positive cases) who underwent radical resection between 2018 and 2022 will be collected. The same digital pathology protocol (QuPath, 500-μm IM band, 1.57 cut-off) will be applied to assess the E/C ratio. The primary objective is to validate the prognostic value of the E/C ratio in HER2-positive patients. Ethical approval is being sought from the participating centers, and data collection is expected to be completed within 6 months. The results will be reported in a separate manuscript.

This study has the following limitations. Firstly, it is a single-center retrospective design with a total sample size of 200 cases, and especially for the HER2-positive subgroup, there are only 35 cases. Post-hoc power analysis based on the observed hazard ratio (high vs. low E/C = 2.48) and the number of events (31 deaths) yielded a statistical power of 59.9% ($\alpha = 0.05$), which is below the conventional 80% threshold. Consequently, even though the difference in median OS between high and low E/C groups was statistically significant ($P = 0.025$), the small sample size and limited power mean that these results should be considered hypothesis-generating rather than definitive. To further assess the robustness of the 1.57 cut-off, we performed a 10-fold cross-validation. The high E/C group showed significantly worse overall survival in only 4 out of 10 folds (Supplementary Table 1), indicating that the prognostic effect is not fully stable. This instability, together with the low statistical power, reinforces the need for external validation. The prognostic role of the E/C ratio in HER2-positive patients requires validation in larger independent cohorts, and we have already initiated an external validation cohort. Future studies need to conduct external validation by combining multi-center, large-sample retrospective cohorts. Secondly, the assessment of TILs currently uses an artificial visual semi-quantitative method. Although two observers independently interpreted and intra-group/inter-group consistency tests were set up, subjective factors still cannot be completely eliminated. The subsequent research plans to develop an automatic segmentation and TILs counting model based on deep learning to further improve the standardization and reproducibility of the assessment. Thirdly, this study only relies on H&E staining to evaluate the total TILs percentage and fails to further distinguish functional subgroups such as $CD8^+$ cytotoxic T cells, $CD4^+$ helper T cells, and $FoxP3^+$ regulatory T cells, nor does it detect more advanced immune response forms such as tertiary lymphoid structures. There is a lack of in-depth analysis of the functional essence of immune rejection. The supplementation of these contents will rely on subsequent multiple immunohistochemical, multi-spectral imaging, or spatial transcriptomics combined analyses. Fourthly, the information on adjuvant chemotherapy is only "yes/no", lacking specific schemes, cycles, and doses, and the control of treatment-related confounding factors is insufficient,

which may cause bias in some prognostic analyses.

Despite these limitations, this study was the first to achieve digital quantification of the spatial heterogeneity of TILs based on conventional H&E sections in gastric adenocarcinoma, and systematically established the associations with HER2 status and survival outcomes, providing preliminary but comprehensive data support for understanding the spatial dimension of the immune microenvironment in gastric cancer.

Conclusion

This retrospective study demonstrates that HER2-positive gastric adenocarcinoma exhibits an "edge-limited" immune phenotype, characterized by an elevated E/C ratio, reduced $CD8^+$ T-cell infiltration, and increased $FOXP3^+$ Treg accumulation. The E/C ratio dichotomized at 1.57 provides significant prognostic stratification for overall survival, an effect that is largely confined to HER2-positive patients (stratified ROC AUCs 0.86-0.86 vs. 0.49-0.57). However, the small sample size in the HER2-positive subgroup (n = 35) yields a statistical power of only 59.9%; therefore, these findings require validation in larger independent cohorts before clinical translation.

Disclosure of conflict of interest

None.

Address correspondence to: Luqing Zhou, Department of Pathology, The First Affiliated Hospital of Lishui University, Lishui People's Hospital, No. 1188 Liyang Street, Yanquan Street, Liandu District, Lishui 323000, Zhejiang, China. Tel: +86-15867079229; E-mail: 15867079229@163.com

References

[1] Shimozaki K, Fukuoka S, Ooki A and Yamaguchi K. HER2-low gastric cancer: is the subgroup targetable? ESMO Open 2024; 9: 103679.

[2] Luo D, Liu Y, Lu Z and Huang L. Targeted therapy and immunotherapy for gastric cancer: rational strategies, novel advancements, challenges, and future perspectives. Mol Med 2025; 31: 52.

[3] Chen Y, Jia K, Chong X, Xie Y, Jiang L, Peng H, Liu D, Yuan J, Li Y, Feng X, Sun Y, Li J, Zhang X and Shen L. Implications of PD-L1 expression on the immune microenvironment in HER2-positive gastric cancer. Mol Cancer 2024; 23: 169.

[4] Angerilli V, Gasparello J, Collesei A, Ceccon C, Bergamo F, Sabbadin M, Parente P, Vanoli A, Niero M, Luchini C, Gafà R, Dei Tos AP, Grillo F, Mastracci L, Lonardi S and Fassan M. Epstein-Barr virus-associated gastric cancer: a histopathologic study with comprehensive molecular profiling. Mod Pathol 2025; 38: 100881.

[5] Wang C, Wang Y, Chen J, Wang Y, Pang C, Liang C, Yuan L and Ma Y. CLDN18.2 expression and its impact on prognosis and the immune microenvironment in gastric cancer. BMC Gastroenterol 2023; 23: 283.

[6] Luo D, Liu Y and Huang L. Advanced therapies for stomach cancer. J Investig Med 2025; 73: 673-684.

[7] Kim R, An M, Lee H, Mehta A, Heo YJ, Kim KM, Lee SY, Moon J, Kim ST, Min BH, Kim TJ, Rha SY, Kang WK, Park WY, Klempner SJ and Lee J. Early tumor-immune microenvironmental remodeling and response to first-line fluoropyrimidine and platinum chemotherapy in advanced gastric cancer. Cancer Discov 2022; 12: 984-1001.

[8] Dienstmann R, Ruiz-García E, Alsina M, Ruiz-Pace F, Groen-van Schooten TS, Martínez-Ciarpaglini C, Fernández-Figueroa EA, Herrera-Goepfert R, Díaz-Romero C, Lino-Silva L, Hernandez-Guerrero AI, Valdez-Reyes NM, León-Takahashi A, Falcón-Martínez JC, Pouw RE, Romero S, Villagrasa R, Cabeza-Segura M, Alarcón-Molero L, Jimenez-Martí E, Miralles A, Boggino H, Gauna C, Pereira R, Lezcano H, Cantero D, Vivancos A, Matito J, Martin A, Gómez M, Castillo E, Vila M, Ferreira RM, Barros R, Santos-Antunes J, Mendes-Rocha M, Costa A, Riquelme E, Roa JC, Latorre G, Freile B, Caro L, Esteso F, O'Connor J, Riquelme A, Owen G, Garrido M, Diez-García M, Figueiredo C, Caballero C, Lordick F, Farrés J, Derks S, Carneiro F, Cervantes A and Fleitas T. Integrated clinicomolecular analysis of gastric cancer in European and Latin American populations: LEGACY project. ESMO Open 2025; 10: 104482.

[9] Choi S and Kim S. Artificial intelligence in the pathology of gastric cancer. J Gastric Cancer 2023; 23: 410-427.

[10] Zhang J, Li Y, Chen J, Huang T, Lin J, Pi Y, Hao H, Wang D, Liang X, Fu S and Yu J. TOB1 modulates neutrophil phenotypes to influence gastric cancer progression and immunotherapy efficacy. Front Immunol 2024; 15: 1369087.

[11] Park JH, Cho HJ, Seo J, Park KB, Kwon YH, Bae HI, Seo AN and Kim M. Genetic landscape and PD-L1 expression in Epstein-Barr virus-associ-

ated gastric cancer according to the histological pattern. Sci Rep 2023; 13: 19487.
[12] Kapoor M, Sehrawat A, Karthik J and Sundriyal D. Tumor infiltrating lymphocytes in gastric cancer: unraveling complex interactions for precision medicine. World J Clin Oncol 2024; 15: 478-481.
[13] Wang B, Du C, Li L, Xie Y, Hu C, Li Z, Zhu Y, Yuan Y, Liu X, Lu N and Xue L. New substituted molecular classifications of advanced gastric adenocarcinoma: characteristics and probable treatment strategies. J Natl Cancer Cent 2022; 2: 50-59.
[14] Weadick CS, Duffy AG and Kelly RJ. Recent advances in immune-based approaches for the treatment of esophagogastric cancer. Expert Opin Emerg Drugs 2022; 27: 19-31.
[15] Scanlon E, Lavery A, Albraikat M, Stevenson L, Kennedy C, Byrne R, Walker A, Mullan-Young B, McManus DT, Virdee PS, Elhussein L, Turbitt J, Collinson D, Miedzybrodzka Z, Van Schaeybroeck S, McQuaid S, James JA, Craig SG, Blayney JK, Petty RD, Harkin DP, Kennedy RD, Eatock MM, Middleton MR, Thomas A and Turkington RC. Immune microenvironment modulation following neoadjuvant therapy for oesophageal adenocarcinoma: a translational analysis of the DEBIOC clinical trial. ESMO Open 2024; 9: 103930.
[16] Attia S, Abd El Hafez A, Abdel-Aziz A, Elmetwaly S and Mokhtar N. Prognostic value of PD-L1 immunohistochemical marker in gastric carcinoma and its correlation with HER2 status. Asian Pac J Cancer Prev 2022; 23: 1433-1444.
[17] Wu L, Luo S, Zhao L, Long A, Li Y and Wang J. Analysis of clinicopathological and molecular characteristics of EBV-associated gastric cancer. Discov Oncol 2025; 17: 6.
[18] Zheng Q and Ge H. The role of mir96 in predicting CTC status and prognostic evaluation in gastric cancer patients. Cell Mol Biol (Noisy-legrand) 2024; 70: 264-274.
[19] Cao J, Hu C, Xu J, Han J, Zhang R, Cao M, Yuan L and Xu Z. Aberrant expression TFR1/CD71 in gastric cancer identifies a novel potential prognostic marker and therapeutic target. Evid Based Complement Alternat Med 2022; 2022: 4257342.
[20] Amirmoezi F and Geramizadeh B. Molecular classification of gastric cancer with emphasis on PDL-1 expression: the first report from Iran. Clin Pathol 2022; 15: 2632010x221096378.
[21] Chen C, Han J, He Q, Yao Q, Wang X, Peng Z, Sun Y, Ji J and Xing X. Tumor-infiltrating immune cell profiles and changes associate with additional trastuzumab in preoperative chemotherapy for patients with HER2-positive gastric cancer. Br J Cancer 2024; 131: 1463-1472.
[22] Chakrabarti J, Koh V, Steele N, Hawkins J, Ito Y, Merchant JL, Wang J, Helmrath MA, Ahmad SA, So JBY, Yong WP and Zavros Y. Disruption of HER2-induced PD-L1 inhibits tumor cell immune evasion in patient-derived gastric cancer organoids. Cancers (Basel) 2021; 13: 6158.
[23] Wang Q, Mao Z, Li W, Wang S, Wang L, Chen L, Yang Z, Fu X, Jiang P, Bai Y, Xu L, Zhang S, Hou Y, Jia X, Jiang L, Liu M, Zhang G, Jiang Y and Guo H. Characteristics of the immunogenicity and tumor immune microenvironment in *HER2*-amplified lung adenocarcinoma. Front Immunol 2022; 13: 1042072.
[24] He J, Kirsche L, Nascakova Z, Manfredi F, Magnani CF, Papa G, Azizi F, Leary P and Müller A. Genetically engineered ErbB2 overexpression sensitizes organoid-derived tumors to checkpoint inhibition in a syngeneic model of gastric cancer. J Immunother Cancer 2026; 14: e012976.
[25] Galon J, Costes A, Sanchez-Cabo F, Kirilovsky A, Mlecnik B, Lagorce-Pagès C, Tosolini M, Camus M, Berger A, Wind P, Zinzindohoué F, Bruneval P, Cugnenc PH, Trajanoski Z, Fridman WH and Pagès F. Type, density, and location of immune cells within human colorectal tumors predict clinical outcome. Science 2006; 313: 1960-1964.
[26] Kim H, Heo YJ, Cho YA, Kang SY, Ahn S and Kim K. Tumor immune microenvironment is influenced by frameshift mutations and tumor mutational burden in gastric cancer. Clin Transl Oncol 2022; 24: 556-567.
[27] Jiang L, Zhao X, Li Y, Hu Y, Sun Y, Liu S, Zhang Z, Li Y, Feng X, Yuan J, Li J, Zhang X, Chen Y and Shen L. The tumor immune microenvironment remodeling and response to HER2-targeted therapy in HER2-positive advanced gastric cancer. IUBMB Life 2024; 76: 420-436.
[28] Janjigian YY, Kawazoe A, Bai Y, Xu J, Lonardi S, Metges JP, Yanez P, Wyrwicz LS, Shen L, Ostapenko Y, Bilici M, Chung HC, Shitara K, Qin SK, Van Cutsem E, Tabernero J, Li K, Shih CS, Bhagia P and Rha SY; KEYNOTE-811 Investigators. Pembrolizumab plus trastuzumab and chemotherapy for HER2-positive gastric or gastro-oesophageal junction adenocarcinoma: interim analyses from the phase 3 KEYNOTE-811 randomised placebo-controlled trial. Lancet 2023; 402: 2197-2208.
[29] Ge S, Wang F, Li H, Yang Y, Zhang L, Duan J, Bai M, Liu R, Ning T, Wang X, Ji Z, Sun Y and Deng T. The combination of anti-PD-1 antibodies, trastuzumab and chemotherapy may improve the outcome of some patients with HER2-positive alpha-fetoprotein-producing gastric can-

cer: a retrospective real-world analysis from a single center. BMC Cancer 2025; 25: 1549.

[30] Yu P, Ding G, Huang X, Wang C, Fang J, Huang L, Ye Z, Xu Q, Wu X, Yan J, Ou Q, Du Y and Cheng X. Genomic and immune microenvironment features influencing chemoimmunotherapy response in gastric cancer with peritoneal metastasis: a retrospective cohort study. Int J Surg 2024; 110: 3504-3517.

[31] Museridze N, Tutisani A, Chabradze G, Beridze N and Muzashvili T. Tumor infiltrating lymphocytes peculiarities in different histopathological and molecular subtypes of gastric carcinoma. Georgian Med News 2021; 165-168.

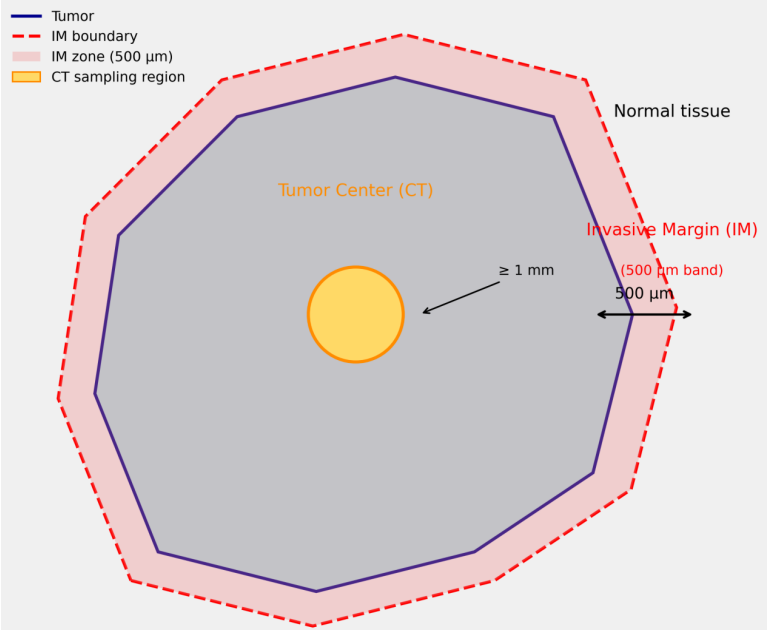

Supplementary Figure 1. Schematic diagram illustrating the definition of the tumor center (CT) and invasive margin (IM). The IM was defined as a 500-μm band centered on the cancer-normal interface (dashed line). The CT was defined as the area located at least 1 mm away from the IM. The yellow circle indicates a representative sampling region for CT-TILs assessment. The double-headed arrow marks the 500-μm width of the IM band. Abbreviation: CT, tumor center; IM, invasive margin; TILs, tumor-infiltrating lymphocytes.

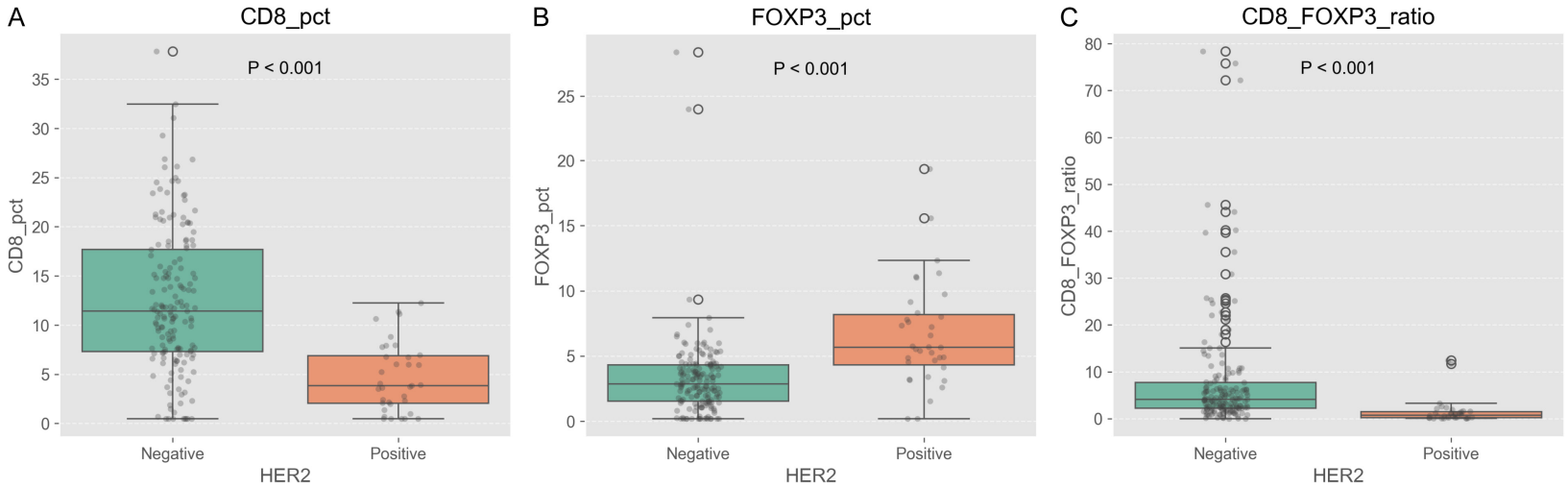

Supplementary Figure 2. HER2 status is associated with distinct CD8⁺ and FOXP3⁺ T-cell infiltration patterns in gastric adenocarcinoma. Boxplots showing (A) CD8⁺ T-cell density, (B) FOXP3⁺ regulatory T-cell density, and (C) the CD8/FOXP3 ratio in HER2-negative (n = 165) and HER2-positive (n = 35) gastric adenocarcinomas. *P* values (two-sided Mann-Whitney U tests) are indicated. HER2-positive tumors had significantly lower CD8⁺ T-cell infiltration (4.67% ± 3.49% vs. 12.48% ± 7.37%, P < 0.001), higher FOXP3⁺ Treg density (6.61% ± 4.07% vs. 3.26% ± 3.16%, P < 0.001), and a markedly reduced CD8/FOXP3 ratio (1.55 ± 2.76 vs. 8.05 ± 12.42, P < 0.001) compared with HER2-negative tumors.

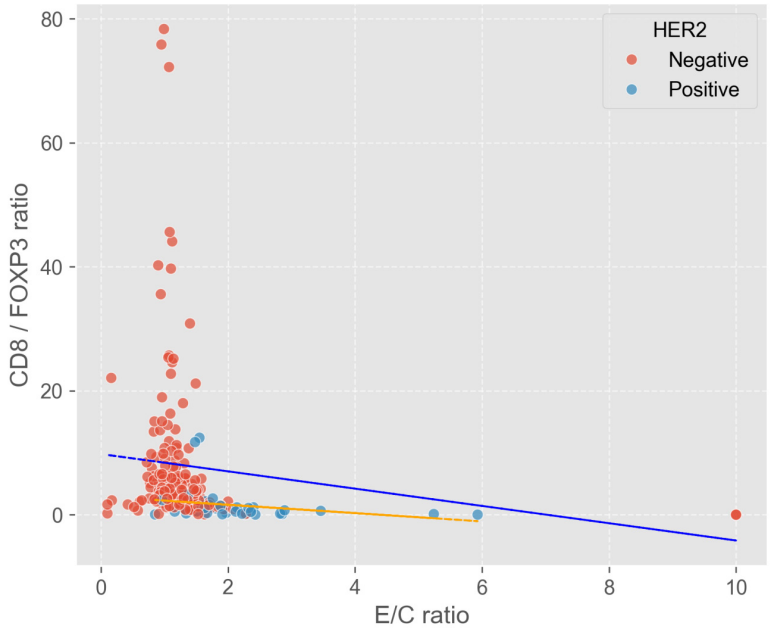

Supplementary Figure 3. The CD8/FOXP3 ratio is inversely correlated with the E/C ratio, especially in HER2-positive tumors. Scatter plot with linear regression lines (dashed) for HER2-negative (blue) and HER2-positive (orange) tumors. Spearman correlation coefficients (ρ) are shown: overall cohort ρ = -0.484 (P < 0.001); HER2-negative ρ = -0.311 (P < 0.001); HER2-positive ρ = -0.470 (P = 0.004). A higher E/C ratio (immune-excluded pattern) is associated with a lower CD8/FOXP3 ratio, indicating an immunosuppressive shift in the tumor microenvironment.

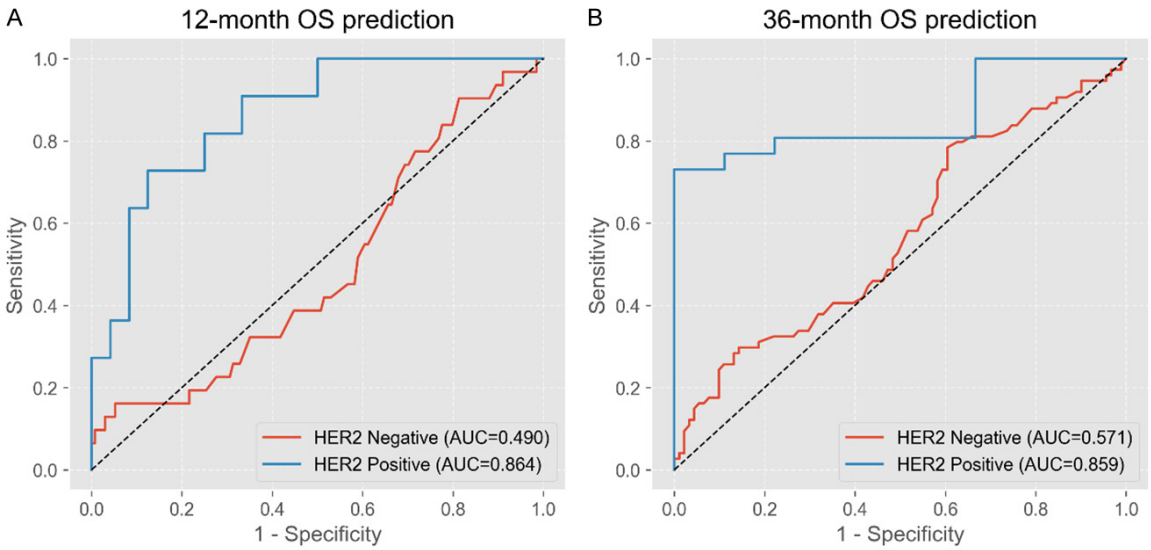

Supplementary Figure 4. Time-dependent ROC analysis demonstrates that the prognostic value of the E/C ratio is largely confined to HER2-positive patients. Time-dependent ROC curves for the E/C ratio predicting (A) 12-month and (B) 36-month overall survival, stratified by HER2 status. Blue: HER2-negative; orange: HER2-positive. AUC values are shown in the legend. The diagonal dashed line represents the reference (AUC = 0.5).

Supplementary Table 1. Ten-fold cross-validation of the 1.57 E/C ratio cut-off for overall survival in the whole cohort (n = 200)

Fold	Log-rank *P* value	Significant (P < 0.05)
1	0.000	Yes
2	0.057	No
3	0.014	Yes
4	0.352	No
5	0.287	No
6	0.001	Yes
7	0.084	No
8	0.458	No
9	0.211	No
10	0.007	Yes

Note: Ten-fold cross-validation using the fixed E/C cut-off of 1.57. The high E/C group showed significantly worse overall survival in 4 out of 10 folds, indicating that the prognostic effect is not fully robust, likely due to the limited sample size.